

The effect of microwave incinerated rice husk ash on the compressive and bond strength of fly ash based geopolymer concrete

Andri Kusbiantoro^{a,*}, Muhd Fadhil Nuruddin^b, Nasir Shafiq^b, Sobia Anwar Qazi^b

^a Faculty of Civil Engineering and Earth Resources, Universiti Malaysia Pahang, Pahang 26300, Malaysia

^b Department of Civil Engineering, Universiti Teknologi Petronas, Perak 31750, Malaysia

HIGHLIGHTS

- ▶ MIRHA is used as the partial replacement for fly ash in geopolymer concrete.
- ▶ It alters the Si/Al in the source material.
- ▶ The elevated temperature presents the optimum curing condition.
- ▶ Improvements on the strengths of fly ash based geopolymer concrete are recorded.

ARTICLE INFO

Article history:

Received 23 April 2011

Received in revised form 12 June 2012

Accepted 13 June 2012

Keywords:

Geopolymer

Fly ash

Rice husk ash

Compressive strength

Bond strength

ABSTRACT

The development of fly ash and microwave incinerated rice husk ash (MIRHA) blend as the source material for geopolymer concrete was studied through the observation of the hardened specimen strength. Compressive and bonding strength of the specimen indicate the significance of curing temperature in the activation of MIRHA particles. The elevated temperature is presenting a suitable condition for rapid dissolution of silicate monomer and oligomer from MIRHA surfaces, which supports the formation of supersaturated aluminosilicate solution in geopolymer system. It contributes to the refinement of pores structure via the increasing geopolymer gel growth, as observed in the consistent compressive strength development of ambient-cured specimen to the oven-cured specimen. Densification of geopolymer framework appears to be the main contributor to the increasing bonding capacity of geopolymer binder.

© 2012 Elsevier Ltd. All rights reserved.

1. Introduction

Geopolymer has progressively enticed many concrete communities around the world due to its revolutionary approach in the production of alternative cement binder. Early research on this material was started in 1957 by Glukhovskiy which was named as “soil cement”, derived from the low basic calcium or calcium-free aluminosilicate (clays) and alkali metal solution used in the cement production [1]. It was Davidovits whom then introduced the first industrial research on “geopolymer” for the development of new binder material using inorganic materials in 1972. Geopolymer term was taken referring to its source material which is a geological origin or by product material that is rich in Silicon and Aluminum. Its reaction product with alkaline solution possessed an amorphous to semi-crystalline three-dimensional silico-aluminate on the material properties [2].

The most prominent source material in geopolymer is coal combustion products, or well known as fly ash. Fly ash is popular due to the amorphous alumina silica content inside and it is abundantly available in many parts of the world. The total amount of fly ash produced in the world has now reached 480 million tons annually, while the total OPC production in the world is reaching 3.3 billion tons in 2010 [3,4]. Based on these numbers, there is an obvious gap between fly ash and OPC production that will contribute to the effectiveness of geopolymer in replacing OPC. Therefore additional source material is imperative, which will reduce these gaps to a lower value.

Rice husk ash is another pozzolanic material that has not been extensively studied in geopolymer application. It is generated from the combustion process of rice husk. Rice husk itself is another issue for environment, due to its abundant amount and capability to resist natural degradation. Total world production of rice husk has reached 130 million tons annually, with 446 thousand tons of them are produced in Malaysia [5]. The current available disposal method is by burning and dumping, which both create environmental pollutions. Therefore this paper studied microwave

* Corresponding author. Tel.: +60 95493009; fax: +60 95492998.

E-mail addresses: andri@ump.edu.my (A. Kusbiantoro), fadhilnuruddin@petronas.com.my (M.F. Nuruddin).

incinerated rice husk ash (MIRHA), an alternative material that has good pozzolanic reactivity, to be included in the geopolymer mixture. MIRHA is produced from the microwave incineration process of rice husk. By utilizing this ash into concrete mixture, it will consume a significant amount of this by-product and contribute to the preservation of environment quality. To provide a robust confirmation in terms of strength performance, geopolymer concrete specimens produced from this combination was assessed via compression and pull out testing, supported by the scanning electron microscope and energy dispersion X-ray analysis.

2. Experimental investigation

2.1. Materials

Fly Ash in this research was obtained from Manjung Coal-Based Thermal Power Plant, Malaysia and categorized as Class F fly ash. Chemical oxide content of fly ash is described in Table 1. Fly ash had the particle size distribution detail as follows: d_{10} at 2.97 μm , d_{50} at 16.54 μm , and d_{90} at 99.21 μm , with BET surface area = 4.26 m^2/g and adsorption average pore width = 41.30 \AA . FESEM image of fly ash particle is presented in Fig. 1a.

Microwave Incinerated Rice Husk Ash (MIRHA) was obtained from the incineration process of rice husk with UTP-Microwave Incinerator in 800 $^{\circ}\text{C}$ incineration temperature. In order to increase its fineness, MIRHA was then ground in ball mill for 2000 cycles. The chemical oxide content of MIRHA is shown in Table 1, with particle size distribution detail as follows: d_{10} at 3.01 μm , d_{50} at 16.76 μm , and d_{90} at 60.53 μm . MIRHA had BET surface area of 67.33 m^2/g and adsorption average pore width of 70.74 \AA . FESEM image of MIRHA particles is presented in Fig. 1b.

MIRHA was introduced in the mixture to replace certain portions of fly ash content as the source material. It was purposed to alter the $\text{SiO}_2\text{-Al}_2\text{O}_3$ ratio in the source material hence improvement on the interfacial transition zone and strength properties of geopolymer concrete were expected. Complete mixture compositions are described in Table 2. Activation of these source materials were completed through the inclusion of sodium hydroxide (NaOH) and sodium silicate (Na_2SiO_3) solution. One kg of 8 M NaOH solution was prepared by diluting 297 gr NaOH pellets with 703 gr water. NaOH solid used was in 99% purities and Na_2SiO_3 had $M_s = 2.0$ (Na_2O : 14.73%; SiO_2 : 29.75%, and H_2O : 55.52%). To prevent the excess heat from NaOH dissolution, these solutions were prepared 1 h before mixing process.

To observe the effect of temperature on the geopolymer concrete properties, three curing regimes were conducted in this research. The geopolymer concrete specimens were exposed to three different conditions, which were ambient, external exposure, and oven curing. In ambient curing, the concrete specimens were placed at the shaded area with maximum temperature 35 ± 1 $^{\circ}\text{C}$. These specimens were constantly protected from direct sunlight and rainfall until the testing days. Meanwhile concrete specimens in external exposure curing were placed in a plastic chamber placed at a non-protected area, exposed to direct sunlight yet protected from rainfall. The maximum temperature in external exposure method reached 55 ± 1 $^{\circ}\text{C}$. All these specimens were kept in their respective curing regime until the testing day. For comparison purpose, strength of hardened specimens was also measured based on the oven curing exposure. Freshly cast specimens were given 1 h delay time before they were placed into the oven. The specimens were placed in electrical oven with temperature 65 $^{\circ}\text{C}$ for 24 h. After 24 h, all specimens in the respective curing conditions were de-moulded and placed back at their initial position, except for oven curing specimens where they were re-placed at the ambient condition.

Geopolymer concrete specimens were then tested on their compressive strength and bonding capacity after 3, 7, and 28 curing days. Pull out test was done to determine the bonding capacity of geopolymer concrete through direct tension force. The pull-out specimen was prepared by setting a steel bar 150 mm into

Table 1
Oxide composition percentage of fly ash and MIRHA particle.

Oxide	Percentage (%)	
	Fly ash	MIRHA
Al_2O_3	29.1	0.45
SiO_2	51.7	89.34
P_2O_5	1.7	2.58
SO_3	1.5	0.90
K_2O	1.6	4.98
CaO	8.84	0.76
TiO_2	0.702	0.02
Fe_2O_3	4.76	0.40
SrO	0.109	–
Mn_2O_3	–	–
MgO	–	0.49

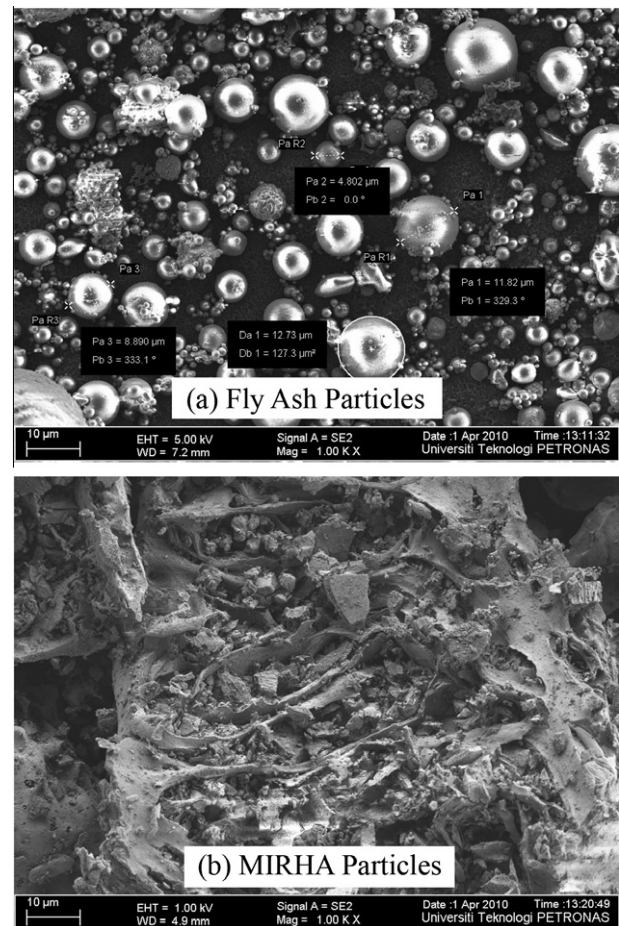


Fig. 1. FESEM images of fly ash and MIRHA particles.

cylindrical cast fresh concrete, with cylinder size 100 mm in diameter and 200 mm in height. This test was conducted on Universal Testing Machine with 2000 kN in capacity. Geopolymer paste specimens were also analyzed for their mineral characterization using energy dispersion X-ray analysis (EDX). Geopolymer paste was selected to minimize the disruption of aggregate particles on the validity of geopolymer framework analysis. For EDX analysis, the data collection was conducted on the crushed geopolymer specimen that was magnified 1000 times in FESEM Zeiss Supra 55VP instruments.

3. Result and discussion

3.1. Compressive strength

Compressive strength development of hardened geopolymer concrete is the basic indicator to the performance of alternative source material, since it provides a fundamental description on the quality of geopolymerization products. Figs. 2–4 show the compressive strength result of hardened geopolymer concrete with 0%, 3%, and 7% MIRHA inclusion respectively. It is obviously presented in these figures how the contribution of MIRHA to the fly ash based geopolymer concrete strength development is limited to certain stage. The increment of temperature from ambient and external exposure curing presents a consistent strength development trend. The excessive amount of water in ambient-cured specimens has hindered the polycondensation process and resulted in a lower compressive strength than external exposure curing. It is a notorious fact that hydroxide activity is significantly affected by the excessive water content in the geopolymer concrete system [6].

The absorptive characteristic of MIRHA reduces the water content in geopolymer system through water absorption mechanism.

Table 2
Detail of mixture proportions.

Mix code	Proportion in kg/m ³							Curing
	Fly ash	MIRHA	Coarse agg	Fine agg	NaOH solution	Na ₂ SiO ₃ solution	Extra water	
A1	350	0	1200	645	41	103	35	Ambient
A2	339.5	10.5	1200	645	41	103	35	
A3	325.5	24.5	1200	645	41	103	35	
B1	350	0	1200	645	41	103	35	External exposure
B2	339.5	10.5	1200	645	41	103	35	
B3	325.5	24.5	1200	645	41	103	35	
C1	350	0	1200	645	41	103	35	Oven
C2	339.5	10.5	1200	645	41	103	35	
C3	325.5	24.5	1200	645	41	103	35	

A rapid transportation of hydroxyl ion on to fly ash particle increases the dissolution of aluminosilicate species and consequently the gelation of supersaturated aluminosilicate solution. Variations in the dissolution and polycondensation rate due to differences in the curing temperature and hydroxide ion activities result in a disparate geopolymer gel production rate. Due to the differences in the solubility degree between fly ash and MIRHA, replacement of fly ash with MIRHA remarkably decreases the dissolution and polycondensation rate of aluminosilicate precursors. However, at a lower gelation rate in ambient curing, the addition of MIRHA contributes to the increasing compressive strength through the reduction on the water filled pores.

Higher surface tension possessed by rough MIRHA particles is understood to trap the moisture from being rapidly dissipated. The water expelled from the geopolymer matrix during polycondensation process is also absorbed by MIRHA specimen and it assists in the formation of discontinuous nano-pores within the matrix. It clarifies the higher strength development retained by MIRHA based geopolymer concrete in ambient curing. The improvement on the compressive strength of MIRHA based geopolymer concrete is up to 22.34% higher than non-MIRHA based specimen in ambient curing. Meanwhile, inclusion of MIRHA in the external exposure curing regime has adversely affected the fly ash based geopolymer concrete strength performance.

An anomaly trend is shown by MIRHA contained specimen when it is exposed to the external exposure curing. Different from ambient curing where MIRHA particles contribute to the compressive strength improvement, in external exposure curing it inconsistently deteriorates the fly ash based geopolymer concrete strength. A barrier appears to prevail in fly ash–MIRHA based geopolymer matrix when the system is exposed to the external exposure curing regime. Rapid dissolution and polycondensation of fly ash in non-MIRHA based geopolymer concrete is completely supported by the elevated temperature. A reduction in the fly ash amount by MIRHA inclusion has delayed the dissolution of aluminosilicate precursors

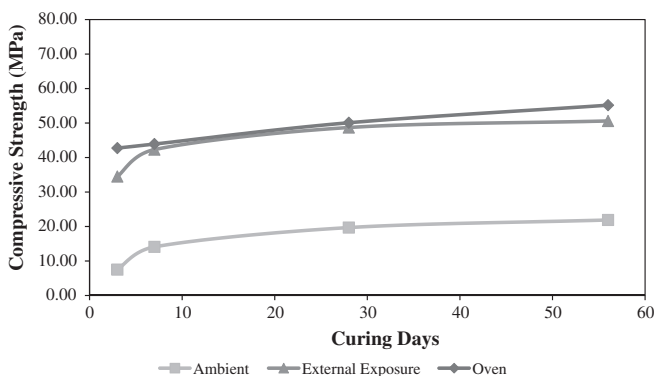


Fig. 2. Compressive strength of fly ash based geopolymer concrete with 0% MIRHA.

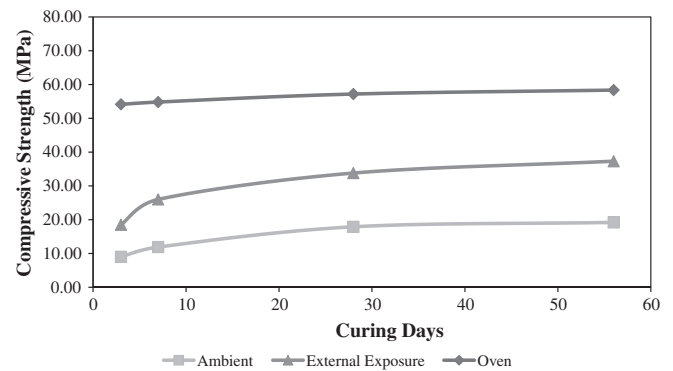


Fig. 3. Compressive strength of fly ash based geopolymer concrete with 3% MIRHA.

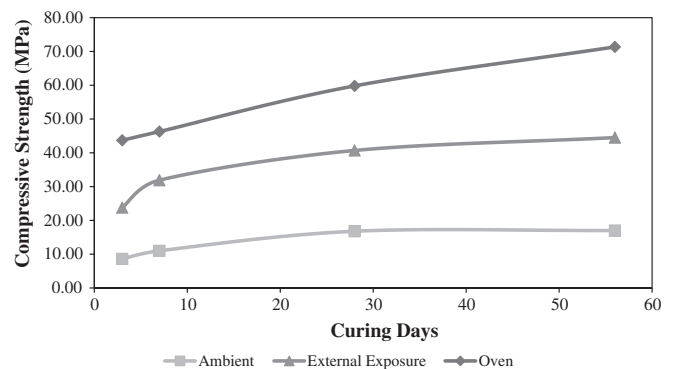


Fig. 4. Compressive strength of fly ash based geopolymer concrete with 7% MIRHA.

from source material which also affected the gelation process of supersaturated aluminosilicate solution. Different silicate feature between MIRHA, fly ash, and soluble silicate has considerably contributed to this condensation process.

It appears that MIRHA particles possess slightly different silicate structure, hence when the SiO₂/Al₂O₃ ratio is altered to a higher ratio; the species of silicate that has large cyclic structure hinders the polycondensation process [7]. It is well understood that in polycondensation, the monomeric Si(OH)₄ and larger linear silicate anions only react with uncomplexed tetrahedral aluminate Al(OH)₄⁻ [8]. The presence of large silicate cyclic structure inhibits the kinetics and reduces the production rate of geopolymer gel. Different from ambient curing, acceleration on the hydrolysis-dissolution-polycondensation process in external exposure-cured specimen is sufficient to fill the existing pores. Rapid dehumidification assisted by the elevated temperature has reduced the disruption of condensation process by the expelled water.

It elucidates the eminence of non-MIRHA based geopolymer concrete over MIRHA based specimens in the performance of

compressive strength development. Non-MIRHA based specimen has the compressive strength 30.60% higher when 3% MIRHA is added to the fly ash based geopolymer system, yet it is reduced to 16.43% in 7% MIRHA based mixture. This trend is then further verified in oven cured specimen since the activation of source material particles is closely related the kinetic energy extracted from elevated temperature [9].

The existence of barrier in MIRHA based system is closely related to the kinetic energy of the reaction. This energy hindrance inhibits further dissolution and condensation process from MIRHA particles. In the following analysis, oven curing regime is added to the evaluation of MIRHA based geopolymer concrete, since activation energy for geopolymer reaction is predominantly supplied by an elevated temperature. As presented in Fig. 4, increasing the curing temperature to 65 °C has significantly improved the MIRHA based geopolymer concrete compressive strength. 3% inclusion of MIRHA in fly ash based geopolymer system has the compressive strength up to 14.17% higher than non-MIRHA based specimen, while 7% inclusion has the strength increment up to 19.41% higher. Elevating the curing temperature has increased the dissolution rate of alumina and silica precursors from glassy fly ash through the polarization of hydroxide ions [6]. Formation of Al–Si rich species in geopolymer system absorbs some of hydrons and increases the amount of hydroxide ions in the solution. With the increasing amount of hydroxide ions, pH of the solution increases and creates further dissolution of aluminosilicate precursors [10].

When fly ash particles are dissolved in water, the Si–O and Al–O bonds on fly ash surface are broken as they are subjected to the polarization effect of OH⁻. Elevated temperature is used to enhance the polarization effect and present more OH⁻ concentration in the solution. At this high concentration, more Si–O bonds from MIRHA surfaces are broken hence rapidly produce supersaturated aluminosilicate solution for further polycondensation process. High dissolution rate of silicate species from MIRHA particles supports the coagulating mechanism of Na⁺ with dissolved monomeric silicate to construct more geopolymer gels hence provide more connectivity in the geopolymer matrix to persist higher external load [11,12].

3.2. Bonding capacity

It is commonly misunderstood that fly ash based geopolymer concrete provides a highly corrosive environment for reinforcement steel, yet in this research the pH range of geopolymer system is of 11.5 to 12.5, slightly different from OPC based concrete where the pH ranges from 12 to 13. Therefore this paper is proposed to verify the null contribution of fly ash based geopolymer concrete to the rapid corrosion of steel reinforcement bar due to the presence of alkali solution.

Impairments on the steel surface due to corrosion are greatly affecting the bonding capacity of concrete binder to the reinforcement bar. Load transfer within concrete system would be disturbed and reinforcement bar might slip out due to friction deficiency between concrete matrices and steel. Therefore, pull out test was performed to provide brief analysis on the protection of reinforcement bar based on the bonding strength point of view, hence reduced the corrosion concern due to alkali activation in fly ash based geopolymer concrete.

Fig. 5 displays the bonding capacity of geopolymer matrix with 3% MIRHA inclusion as the additional source materials cured in ambient temperature condition. Inclusion of MIRHA in this specimen has significantly improved the bonding strength between geopolymer matrix and steel reinforcement bar up to 38.31% higher than control specimen without MIRHA inclusion. In low temperature curing, precipitation of silicate species along with the increasing MIRHA content has a contribution to the refinement of

geopolymer matrix pores structure for pull out strength. Nevertheless, since silicate precursors only precipitate instead of involve in further polycondensation process, it does not provide significant contribution to the geopolymer concrete compressive strength.

Increasing curing temperature to the external exposure condition has presented a general escalation to the performance of geopolymer matrix bonding strength, as shown in Fig. 6. In average, external exposure specimen presents the bonding strength up to 73.23% higher than ambient cured specimens. Rapid growth of geopolymer gel due to higher nucleation rates of dissolved aluminosilicate precursors followed by immediate polycondensation of supersaturated aluminosilicate solution has increased the density of geopolymer matrix in the specimen. It produces more uniform confinement and stiffness to the geopolymer concrete system, hence increases the bonding strength between steel bar and geopolymer matrix. Even though MIRHA inclusion consistently has bonding strength lower than non-MIRHA specimen in the external exposure condition, yet 7% MIRHA inclusion presents only 4.29% lower bonding strength than non-MIRHA specimen.

Additional observation on the characteristic of geopolymer concrete bonding strength is done with the supplementary data from oven cured specimen. In oven-cured specimen, the bonding strength increases rapidly in the first curing week and started to stable afterward, as presented in Fig. 7. This remaining reaction, after 24 h oven curing, is originated from further dissolution-condensation process at a lower rate and diffusion of remaining precursors with fly ash particles to reach an equilibrium condition [13]. The densification of geopolymer gel appears to be affected by several factors, such as the reactivity of source material, access to the elevating temperature, and alkali activation system used. The unreacted fly ash particle, particularly in the elevated-temperature condition contains a non-amorphous (i.e. crystalline or semi-crystalline) structure that decreases the particles dissolution rate. Once the reactive parts of fly ash particles are completely dissolved, the production of aluminosilicate gel will be significantly interrupted. It explains the less-diverging bonding strength results of fly ash–MIRHA based geopolymer concrete cured in oven regime.

Reduction on the amount of fly ash reactive alumina by the inclusion of reactive silica from MIRHA particles is significantly supported by the elevated temperature in oven curing. Rapid dissolution of Si–O bonds from MIRHA surfaces has sufficiently contributed to polycondensation process of geopolymer gels. Adequate amount of geopolymer gels produced from Si–O bond species (siloxo, siloxonate, and silanol) fills the nanopores in geopolymer matrix and creates more confinement in the hardened concrete specimen. The balance production of Si and Si–Al based geopolymer link has presented a comparable bonding strength results even with the inclusion of MIRHA as the additional source

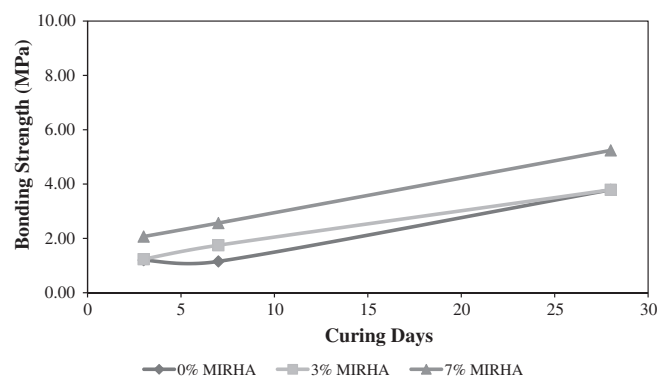


Fig. 5. Bonding strength of fly ash–MIRHA based geopolymer concrete in ambient curing.

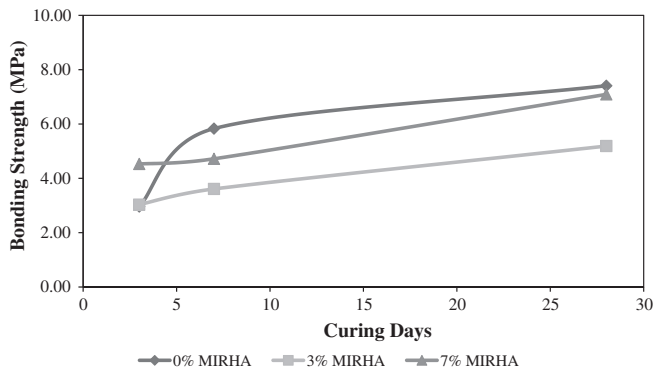


Fig. 6. Bonding strength of fly ash-MIRHA based geopolymer concrete in external exposure curing.

material. The activation of fly ash-MIRHA based geopolymer concrete with alkaline solution is also verified as a non-destructive material to the passivity layer of embedded steel reinforcement.

3.3. Field emission scanning electron microscope analysis

Microstructure study is a constructive method to support the strength analysis since the quality of pores within geopolymer matrices is affecting the capability of geopolymer concrete to sustain and distribute the external loads.

In this research, qualitative analysis of geopolymer concrete microstructure was completed through the Field Emission Scanning Electron Microscopy (FESEM) investigation. Fig. 8 shows the FESEM appearance of geopolymer matrix in fly ash-MIRHA based system under ambient curing regime. The product of low dissolution and polycondensation rate due to energy deficiency for reaction kinetics is obviously shown in Fig. 8. The porous geopolymer matrix structure due to insufficient growth of geopolymer gel resulted in a low capability of ambient-cured specimens to transfer external load within geopolymer concrete system hence created a low strength geopolymer concrete specimen. Instead of condensate into aluminosilicate gels, the dissolved alumina and silica species precipitate on fly ash particles and into porous geopolymer matrix. Therefore, even though the external appearance of this geopolymer concrete indicates a properly set specimen, yet their matrix connectivity is weak due to insufficient geopolymer gel.

In Fig. 8a, it shows the appearance of fly ash that is covered and bonded with aluminosilicate gels. Denser coverage of these gels creates a better connection system to transfer external load within geopolymer concrete specimen. It explains the declining trend of compressive strength in ambient cured specimen. Disconnection

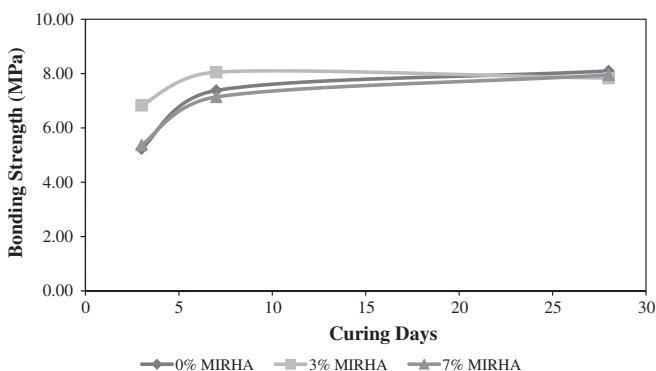


Fig. 7. Bonding strength of fly ash-MIRHA based geopolymer concrete in oven curing.

in the load transferring system had created a premature failure to the geopolymer concrete before it reached the ultimate strength. This premature failure is typically triggered by the presence of excessive void or crack path.

A loaded crack path is connected to the other crack paths through voids or pores due to weak interlink in the concrete matrix. A refinement in these pores or crack paths by denser geopolymer matrix will significantly improve concrete strength performance. However, since geopolymer system in the low temperature curing regime does not provide a denser matrix to cover these pores, the low temperature-cured specimen does not present higher compressive strength than the elevated temperature-cured specimens. Alteration on the $\text{SiO}_2/\text{Al}_2\text{O}_3$ of source material by adding MIRHA to replace certain amount of fly ash is not followed by rapid production of aluminosilicate gels networks due to deficiency in the dissolution and polycondensation process. They are obviously shown in Fig. 8b and c, where the unreacted fly ash particle is loosely connected by porous geopolymer matrix resulted from precipitation of dissolved species.

In terms of interfacial transition zone (ITZ) characteristic, the gap detected is varied for each MIRHA inclusion. As shown in Fig. 8d–f, 7% MIRHA inclusion in ambient curing presents the weakest zone with average gap size detected of $16.10\ \mu\text{m}$. This opening is rectified in 3% MIRHA inclusion with the average detected gap of $0.99\ \mu\text{m}$, and control specimen with 0% MIRHA has the narrowest opening with $0.56\ \mu\text{m}$ gap. These conditions are caused by slower dissolution rate of Al and Si monomer from source material. As it has been explained in strength properties analysis, MIRHA appears to be less dissolvable. Therefore, at low temperature, Si bonds on MIRHA surfaces are difficult to be broken. Fewer amount of Si and Al monomers extracted due to replacement of fly ash with MIRHA, and deficiency in Si species from dissolution process of MIRHA has the fly ash-MIRHA based geopolymer concrete to perform at their low level.

The appropriate amount of heat to overcome the high requirement of reaction kinetic in alkali activated geopolymer concrete is properly represented by external exposure curing regime. Dissolution of source material is immaculately done as indicated by few unreacted fly ash particles in Fig. 9. Aluminosilicate gels produced from the reaction are also appropriately dispersed and occupy the existing pre-water-filled voids. However different dissolution rate between blended and unblended source material has resulted in different geopolymer matrix density. Non-MIRHA specimen has denser geopolymer matrix than MIRHA based specimens, as indicated by fewer pores observed in the geopolymer matrix in Fig. 9a than pores volume in Fig. 9b and c. The higher porosity of geopolymer concrete matrix reduces the capability of geopolymer concrete system to sustain and distribute the external load properly. It explains the declining trend of compressive strength in external exposure curing for fly ash-MIRHA based specimens.

The appearance of large ITZ opening in external exposure specimens is scarcely detected. Fig. 9d–f shows the gap is completely covered with geopolymer matrices in all three specimens. The difference between the specimens is the porosity state of geopolymer matrices. It explains the higher mechanical strength of external exposure specimens than ambient specimens. Since concrete failure due to compressive load is commonly triggered by the existence of micro crack in ITZ, perfect bonding between geopolymer paste and aggregate enhances the load distribution within the concrete system and blocks the crack path, thus resulting in higher compressive strength.

As a comparison, FESEM of fly ash-MIRHA based specimen cured with oven curing is presented in Fig. 10 to provide clear vision on the appearance of geopolymer gel from gelation process. Due to rapid geopolymerization process, both fly ash and fly ash-MIRHA based specimen are displaying similar FESEM image

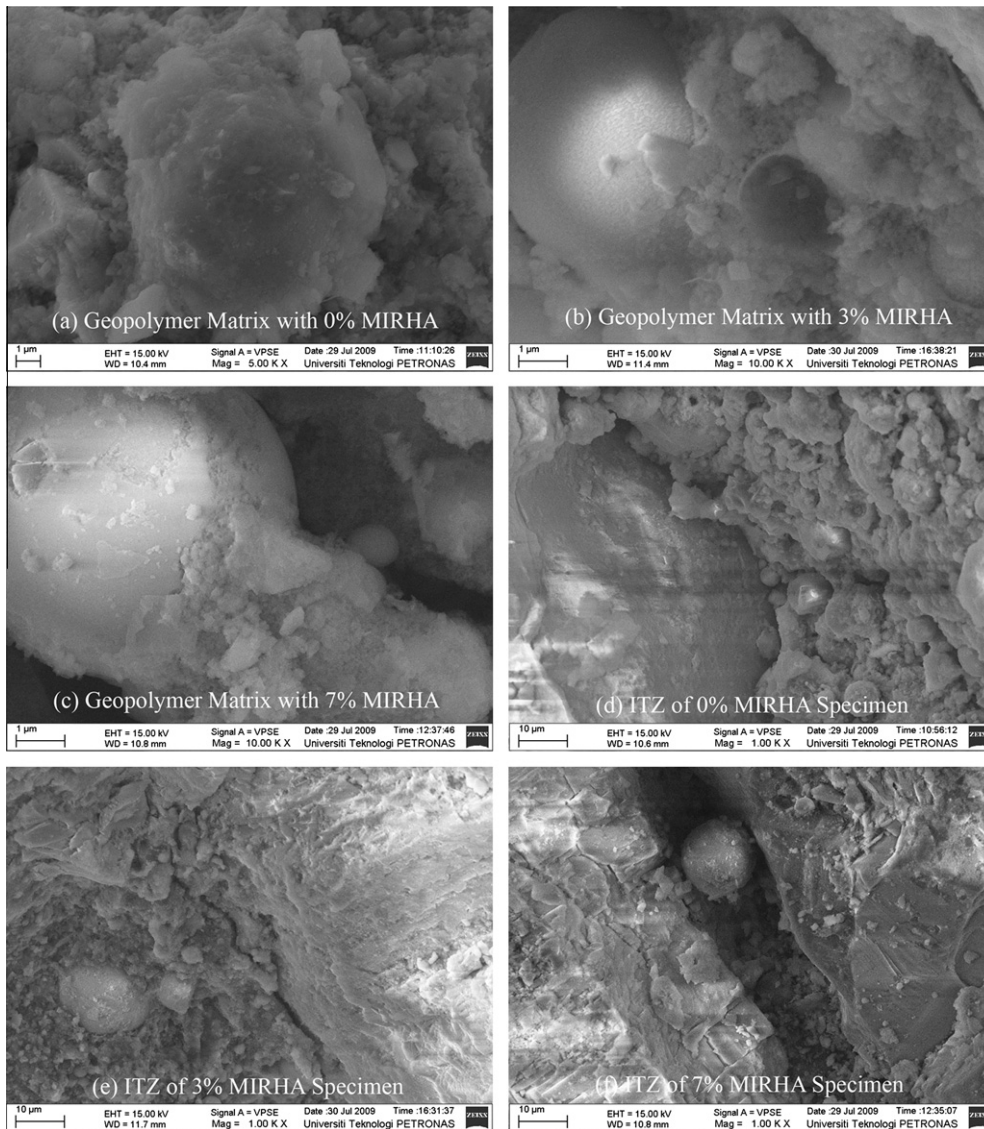


Fig. 8. FESEM images of geopolymer concrete cured in ambient condition.

characteristics. Therefore, a group of images representing both source materials is selected based on the area of observation similarity and level of image quality, i.e. geopolymer matrix and ITZ part. It has been explained that oven curing provides a suitable condition to accelerate the geopolymeric reaction. The optimum reaction kinetic transforms the aluminate and silicate monomers from geopolymer precursor into amorphous aluminosilicate gel and nano-crystalline “zeolitic” phase. Nevertheless, it appears that fly ash and MIRHA used in this research contain some unreactive materials. These unreactive materials were not involved in the geopolymerization process hence the system produced excess sodium on the specimen surface. These prism-like crystals can be observed in Fig. 10a, meanwhile in Fig. 10b–d geopolymeric (nano) micelles that construct the polymeric gel structure are detected at the geopolymer matrix. Silicate and aluminate precursors from fly ash and MIRHA are transformed into the aluminosilicate gel networks and present a significant improvement to the aggregate–geopolymer matrix connectivity. Complete dissolution of fly ash implies to the formation of supersaturated aluminosilicate solution hence results in a higher further nucleation and polycondensation rates.

Formation of this nano structure holds the responsibility in bridging all geopolymer concrete components to produce a dense

and strong geopolymer concrete structure. As observed in the FESEM images, the homogeneity level of oven and external exposure-cured geopolymer matrix is slightly higher than ambient cured specimens. The high dissolution rate in the elevated temperature curing methods is added with the diffusion of remaining ions and partially reacted fly ash at a lower rate to reach the equilibrium condition. The geopolymer gel produced from the reaction serves as the binding material that fills pre-water-filled voids and connects the aggregate and geopolymer matrix with a distinctive micelles formation.

3.4. EDX characterization

The specimen representatives were selected from each curing condition with MIRHA additions at 0% and 7%. The result of EDX analysis for ambient cured specimen is presented in Table 3. From these results, element of Si, Al, Na, Fe, Ca, and O appear to be the dominant elements in fly ash–MIRHA based geopolymer framework. In ambient curing, the Si/Al ratio has a decreasing trend from 3 curing days to 28 curing days, as shown in Table 3. At 3 curing day specimen, Si/Al ratio detected is 2.41 for fly ash based specimen, and 2.86 for fly ash–MIRHA based specimen. The difference

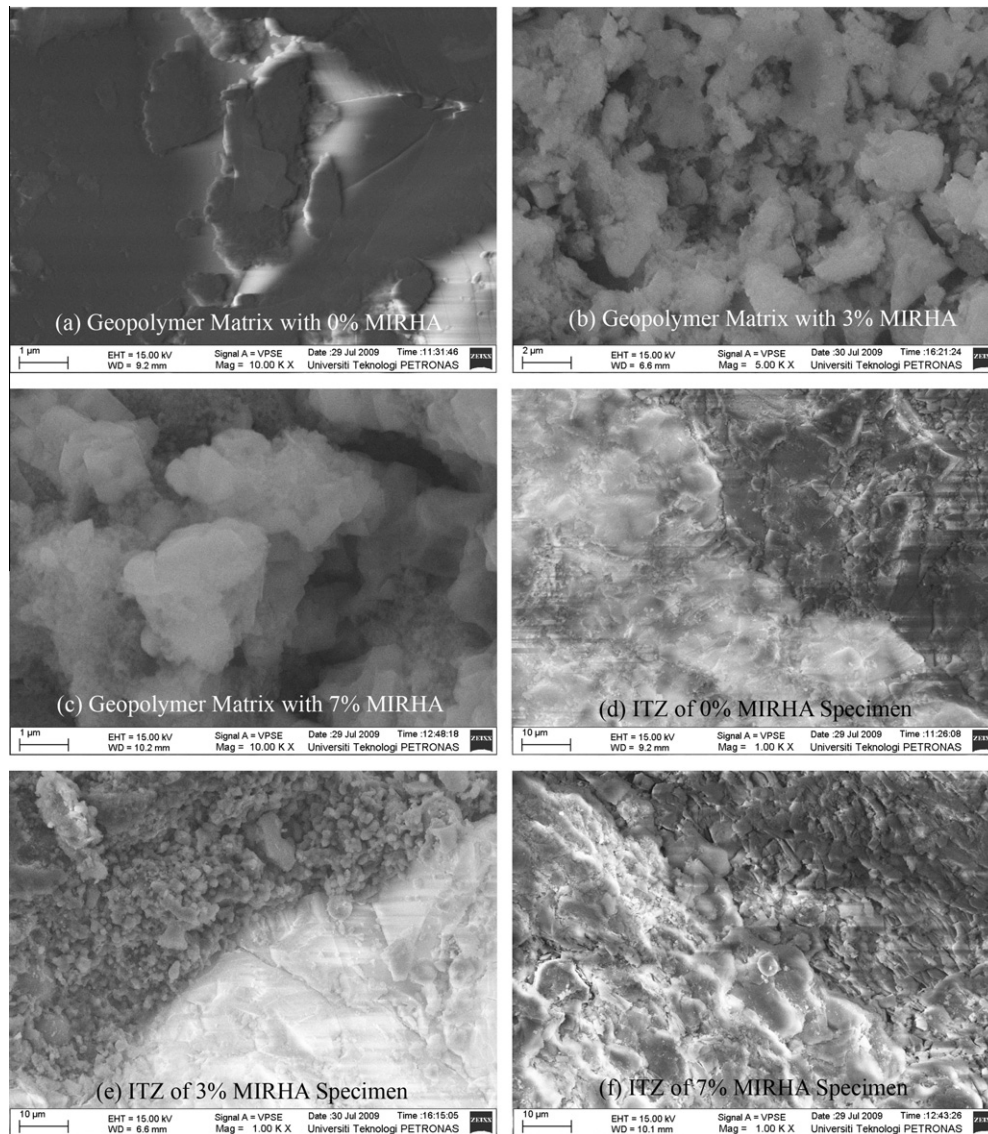


Fig. 9. FESEM images of geopolymer concrete cured in external exposure condition.

occurs due to the dissolution of silica particles and the remained unreactive silica particle at MIRHA surfaces. These values consistently decrease to 1.61 for fly ash based specimen and 2.21 for fly ash–MIRHA based specimen after 28 days of curing. It justifies the simultaneous reaction of alumina and silica precursor's dissolution–polycondensation process in geopolymer framework and consistent low rate diffusion of residual ions with fly ash particle to reach an equilibrium condition. An anomaly is detected at the fly ash–MIRHA based specimen after 7 days of curing. An extremely high Si/Al ratio (13.97) is spotted in the EDX analysis. It appears that high precipitation of dissolved silica precursors and unreactive silica particles on MIRHA surfaces due to low geopolymer system reactivity significantly contributes to the anomaly of this EDX analysis.

Meanwhile, as shown in Table 4, the external exposure-cured specimen has an increasing Si/Al ratio within the observation period (3–28 days of curing). After three days of curing, Si/Al ratio observed in the specimen is 2.46 for fly ash based specimen and 3.14 for fly ash–MIRHA based specimen. After 28 days of curing, Si/Al ratio of geopolymer paste specimen constantly increases to 2.95 for fly ash based specimen and 4.24 for fly ash–MIRHA based specimen. The increasing curing temperature in this condition has

significantly accelerated the dissolution and polycondensation of aluminosilicate gel in geopolymer framework, hence the absorption of hydrogen ion (H^+) by these Al–Si-rich layers contributes to the further dissolution of silica species from MIRHA surfaces due to the increasing pH of solution.

This process is well-presented in the Si/Al ratio analysis of fly ash–MIRHA based geopolymer paste where the ratio has significantly increased from 2.21 to 4.24 when the curing temperature raised from ambient to external exposure condition. In addition to this trend, the amount of Ca in geopolymer matrix is also proportionally intensified with the elevating curing temperature condition. Ca–O has a weaker bond than Si–O and Al–O bonds, therefore alteration on the reaction kinetics due to elevating temperature has dissolved more Ca–O species from fly ash particles [14].

In oven curing condition, Table 5 shows a different trend between fly ash based specimen and fly ash–MIRHA based specimen. In fly ash based specimen, 2.35 Si/Al ratio in 3 days specimen decreases to 1.24 after 28 days of curing. Meanwhile in fly ash–MIRHA based specimen, 2.97 Si/Al ratio in 3 days specimen increases to 4.44 after 28 days of curing. The declining trend of Si/Al ratio in fly ash based specimen emerges from the rapid dissolution of alumina species from fly ash particles. The dissolution of aluminum

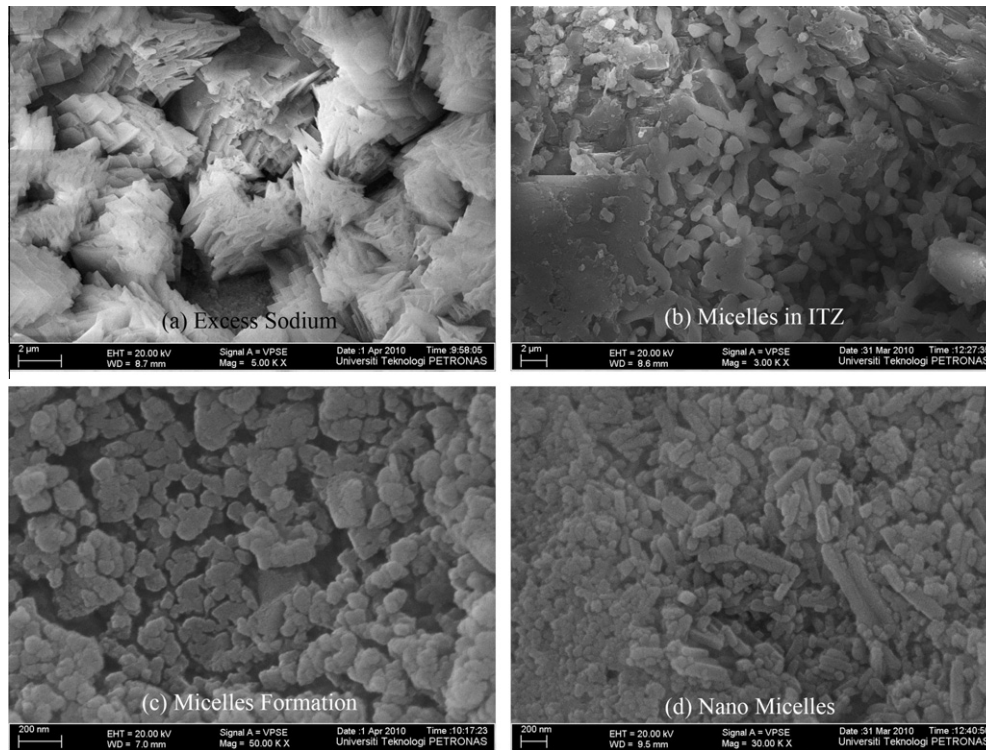


Fig. 10. FESEM images of geopolymer concrete cured in oven.

Table 3
EDX element weight percentage analysis of ambient cured specimens (wt.%).

Element	0% MIRHA			7% MIRHA		
	3 days	7 days	28 days	3 days	7 days	28 days
O	59.23	59.68	62.24	61.52	53.15	59.41
Na	8.42	12.45	6.73	8.58	3.56	7.52
Mg	2.04	3.05	0.98	1.65	0.58	2.70
Al	8.46	9.25	13.19	8.04	2.74	8.81
Si	20.46	13.78	21.25	23.01	38.29	19.46
S	0.67	0.64	0.47	0.72	0.26	0.22
K	0.94	0.48	0.83	1.21	0.68	0.71
Ca	5.91	5.28	4.31	5.63	2.17	5.62
Ti	0.50	0.30	0.59	0.54	0.00	0.36
Fe	4.08	3.19	2.41	4.08	1.54	3.24

Table 4
EDX element weight percentage analysis of external exposure cured specimens (wt.%).

Element	0% MIRHA			7% MIRHA		
	3 days	7 days	28 days	3 days	7 days	28 days
O	59.27	59.09	56.39	61.44	59.24	57.08
Na	7.51	5.76	6.88	9.42	7.55	5.79
Mg	1.75	1.10	1.22	1.80	1.55	1.25
Al	8.81	15.33	8.35	7.61	7.75	5.79
Si	21.67	24.00	24.6	23.9	23.41	24.57
S	0.43	0.00	0.26	0.54	0.46	0.59
K	1.00	2.09	1.47	1.26	1.39	1.04
Ca	5.68	2.82	4.59	6.22	7.19	11.86
Ti	0.60	0.79	1.36	0.47	0.47	0.47
Fe	4.85	3.06	3.76	5.12	4.26	3.59

happens at higher rate than silicon during the early stage of geopolymerization [15]. Sufficient amount of constant heat during the curing process has accelerated the dissolution and nucleation process of these alumina species, hence results in a higher

Table 5
EDX element weight percentage analysis of oven cured specimens (wt.%).

Element	0% MIRHA			7% MIRHA		
	3 days	7 days	28 days	3 days	7 days	28 days
O	61.52	57.68	61.73	60.62	52.41	56.93
Na	8.68	6.96	4.3	8.48	8.57	8.18
Mg	1.96	1.79	0.69	1.28	1.13	1.55
Al	9.15	10.04	18.13	7.54	8.65	5.48
Si	21.46	20.57	22.48	22.39	25.3	24.35
S	0.49	0.00	0.00	0.27	0.41	0.37
K	1.16	1.06	0.89	1.11	1.19	1.00
Ca	6.42	13.18	3.06	5.33	5.4	7.68
Ti	0.76	0.73	0.25	0.64	0.4	0.55
Fe	5.09	12.85	1.77	3.26	3.38	7.90

concentration of Al in geopolymer matrix than ambient and external exposure specimens.

Meanwhile, in fly ash–MIRHA based specimen, dissolution of silica species from MIRHA particles consistently contributes to the increasing Si/Al ratio trend for fly ash–MIRHA based specimens. The formation of these Si–O based geopolymer networks has resulted in a denser geopolymer paste, hence provides better bonding at the interfacial transition zone and nanopores structure of geopolymer matrix. It supports the analysis of higher strength possessed by fly ash–MIRHA based specimen in oven curing.

In general, based on the ratio of Si/Al and Na/Al, there are three types of geopolymer structures observed in this research according to the empirical formula proposed by Davidovits [2]:



where M represents a cation such as Sodium (Na), Potassium (K), or Calcium (Ca); n is the degree of polycondensation; $z = 1, 2, 3$ or higher; and w is the amount of binding water.

These three types of geopolymer structure are formulated based on the ratio which extends from 1–3 and 0.4–1 for Si/Al and Na/Al respectively:

1. Poly(sialate), i.e. $\text{Na}_n\text{-(Si-O-Al-O)}_n\text{-}$
2. Poly(sialate-siloxo), i.e. $\text{Na}_n\text{-(Si-O-Al-O-Si-O)}_n\text{-}$
3. Poly(sialate-disiloxo), i.e. $\text{Na}_n\text{-(Si-O-Al-O-Si-O-Si-O)}_n\text{-}$

Mixtures with Na/Al ratio less than one indicate an insufficiency of sodium as cation, thus another cation is needed to balance the covalent bonding. There is also possibility of Ca species to react and form calcium silicate hydrate (C-S-H) gels in the geopolymer system [16].

4. Conclusion

Based on the result of these analyses, it can be concluded that MIRHA significantly contributes to the formation of geopolymer matrix, particularly when geopolymer system is entirely supported by an elevating temperature during the maturing process. Additional dissolution and polycondensation process of aluminate precursors from fly ash particles with silicate monomer and small oligomer supplied by MIRHA particles has resulted in a higher geopolymer matrix quality with denser gel structure, hence capable to improve the performance of fly ash based geopolymer concrete. Denser gel structure presents a higher connectivity in the load distribution system among geopolymer concrete framework, for example: interfacial of aggregate-geopolymer paste, interfacial of reinforcement bar-geopolymer paste, and micro/nano-pores in geopolymer matrix.

Acknowledgments

The authors appreciate the financial and instrument supports received from Universiti Malaysia Pahang and Universiti Teknologi Petronas.

References

- [1] Glukhovskiy VD. Soil silicates (Gruntosilikaty). USSR Kiev: Budivelnik Publisher; 1959.
- [2] Davidovits J. Geopolymer chemistry and application. Institut Geopolymere; 2008.
- [3] H.J. Feuerborn and European Coal Combustion Products Association e.V. Coal ash utilisation over the world and in Europe. In: Workshop on environmental and health aspects of coal ash utilization; 2005.
- [4] Oss HGV. Cement. United States Geological Survey: Mineral Commodity Summaries 2011.
- [5] IRRI and FAOSTAT database. World rice statistics – paddy rice production. International Rice Research Institute; 2008.
- [6] Teoreanu I. The interaction mechanism of blast-furnace slags with water: the role of activating agents. *Il Cemento* 1991;8(2):91–7.
- [7] Swaddle TW. Silicate complexes of aluminium (III) in aqueous systems. *Coord Chem Rev* 2001;219–221:665–86.
- [8] Harris RK, Maybodi AS, Smith W. The incorporation of aluminium into silicate ions in alkaline aqueous solutions, studied by aluminium-27 n.m.r. *Zeolites* 1997;19:147–55.
- [9] Fernández-Jiménez A, Palomo A, Sobrados I, Sanz J. The role played by the reactive alumina content in the alkaline activation of fly ashes. *Micropor Mesopor Mater* 2006;91:111–9.
- [10] Rajaokarivony-Andriambololona Z, Thomassin JH, Baillif P, Touray JC. Experimental hydration of two synthetic glassy blast furnace slags in water and alkaline solutions (NaOH and KOH 0.1 N) at 40 °C structure composition and origin of the hydrated layer. *J Mater Sci* 1990;25:2399–3410.
- [11] Wijnens PWJG, Beelen TPM, de Haan JW, van de Ven LJM, van Santen RA. The structure directing effect of cations in aqueous silicate solutions. A ²⁹NMR study. *Colloids Surf* 1990;45:255–68.
- [12] Dent Glasser LS. The gelation behavior of aluminosilicate solutions containing Na⁺, K⁺, Cs⁺, Me₄ⁿ⁺. *J Chem Soc, Chem Commun* 1984;19:1250–2.
- [13] Sindhunata, van Deventer JSJ, Lukey GC, Xu H. Effect of curing temperature and silicate concentration on fly-based geopolymerization. *Ind Eng Chem Res* 2006;45:3559–68.
- [14] Shi C, Krivenko PV, Roy D. Hydration and microstructure of alkali-activated slag cements. In: *Alkali-activated cements and concrete*. Oxford: Taylor and Francis; 2006. p. 66.
- [15] Pietersen HS, Fraay ALA, Bijen JM. Reactivity of fly ash at high pH. *MRS Proc* 1989;178:139–57.
- [16] Guo X, Shi H, Dick WA. Compressive strength and microstructural characteristics of class C fly ash geopolymer. *Cement Concr Compos* 2010;32:142–7.